

Stereochemical Control of Nonamphiphilic Lyotropic Liquid Crystals: Chiral Nematic Phase of Assemblies Separated by Six Nanometers of Aqueous Solvents

Sijie Yang,[†] Bing Wang,[‡] Dawei Cui,[†] Deborah Kerwood,[†] Stephan Wilkens,[§] Junjie Han,[†] and Yan-Yeung Luk^{*,†,||}

[†]Department of Chemistry, Syracuse University, Syracuse, New York 13244, United States

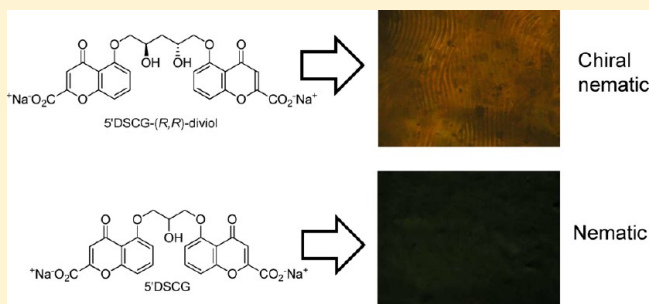
[‡]Novartis Institutes for BioMedical Research, Inc., Cambridge, Massachusetts 02139, United States

[§]Department of Biochemistry and Molecular Biology, Upstate Medical University, State University of New York, Syracuse, New York 13210, United States

^{||}Department of Biomedical and Chemical Engineering, Syracuse University, Syracuse, New York 13244, United States

S Supporting Information

ABSTRACT: Unlike conventional thermotropic and lyotropic liquid crystals, nonamphiphilic lyotropic liquid crystals consist of hydrated assemblies of nonamphiphilic molecules that are aligned with a separation of about 6 nm between assemblies in an aqueous environment. This separation raises the question of how chirality, either from chiral mesogens or chiral dopants, would impact the phase as the assemblies that need to interact with each other are about 6 nm apart. Here, we report the synthesis of three stereoisomers of disodium chromonyl carboxylate, 5'DSCG-diviol, and the correlation between the molecular structure, bulk assembly, and liquid crystal formation. We observed that the chiral isomers (enantiomers 5'DSCG-(*R,R*)-diviol and 5'DSCG-(*S,S*)-diviol) formed liquid crystals while the achiral isomer 5'DSCG-*meso*-diviol did not. Circular dichroism indicated a chiral conformation with bisignate cotton effect. The nuclear Overhauser effect in proton NMR spectroscopy revealed conformations that are responsible for liquid crystal formation. Cryogenic transmission electron microscopy showed that chiral 5'DSCG-diviols form assemblies with crossings. Interestingly, only planar alignment of the chiral nematic phase was observed in liquid crystal cells with thin spacers. The homeotropic alignment that permitted a fingerprint texture was obtained only when the thickness of the liquid crystal cell was increase to above $\sim 500\ \mu\text{m}$. These studies suggest that hydrated assemblies of chiral 5'DSCG-diviol can interact with each other across a 6 nm separation in an aqueous environment by having a twist angle of about 0.22° throughout the sample between the neighboring assemblies.



INTRODUCTION

The effect of how chiral molecules influence molecular assembly is of continuous interest.^{1–5} However, the effect of how chiral molecules influence solvent organization and phase behavior of a lyotropic system is intriguing and less well understood.^{6–13} The most intriguing aspect is that as lyotropic liquid crystals are formed by organized assemblies of molecules in a solvent, the effect of chiral dopants or chiral mesogens on the assembly, if any, must transmit across the aqueous solvent between assemblies and pivot the orientation of the assembly as a whole.^{12,13} In principle, this effect may or may not transmit throughout the whole sample. In case the effect is continuous throughout the assemblies, a cholesteric phase is obtained.⁹

In particular, the molecular assemblies of nonamphiphilic molecules in water give rise to the traditionally called chromonic liquid crystals^{14–31} consisting of hydrated assemblies of nonamphiphilic molecules aligned with a separation of

5–6 nm in water.^{22,32} These molecular assemblies are remarkable considering the large volume of water, yet the liquid crystal properties are similar to conventional thermotropic liquid crystals with regard to birefringence¹⁶ and temperature dependence of phase transitions.^{15,22} This unique molecular assembly also raises the question of how the molecular organizations are influenced by chiral dopants or chiral mesogens. For these lyotropic chromonic liquid crystals, if the chiral mesogens or added chiral dopants were to have an impact on the organization of the molecular assemblies, there must exist a mechanism for how each assembly is influenced by the chiral environment created by the neighboring assemblies 6 nm away. How the chiral dopants or chiral mesogens impact

Received: February 7, 2013

Revised: April 27, 2013



the water solvation surrounding the assemblies and influence the neighboring assemblies 5–6 nm away is unclear. There are few reports on chiral mesogens that form a chromonic liquid crystal phase, but several reports examined chromonic liquid crystal phases influenced by chiral dopants that would have an interaction over 6 nm between the assemblies.^{14,33,34,61} A review on chromonic liquid crystals also showed three chiral chromonic mesogens, two of which have been demonstrated to show fingerprint texture.²⁰

Here, we report the synthesis of three stereoisomers of disodium chromonyl carboxylates connected by a diviol linker, 5'DSCG-diviol (Figure 1), and demonstrate a strong

correlation among molecular structures, assembly properties, and the chiral nematic phase that requires chemical communication between the molecular assemblies, separated by a distance of 5–6 nm of the aqueous solvent.

RESULTS AND DISCUSSION

Design and Synthesis of the Stereoisomers of 5'DSCG-Diviols. The generic 5'DSCG molecule (Figure 1) in water exhibits a wide range of liquid crystal properties that are unmatched by conventional lyotropic liquid crystals that are made of amphiphilic molecules.^{15,16,22} For instance, 5'DSCG is not amphiphilic but forms a liquid crystal phase in water.²² We note that while the thread model is consistent with the requirement for a divalent molecule for forming a liquid crystal phase,²² it is not consistent with a H-stacking model.³⁵ Here, we use the generic term assembly to describe the molecule interaction at concentrations lower than liquid crystal formation. Several other fused aromatic dye-based molecules also form assemblies and lyotropic liquid crystals in water, but 5'DSCG forms liquid crystal phases at lower concentration with higher birefringence compared to other dye-based molecules.¹⁶ To explore the structural requirement for liquid crystal phase formation, we recently screened a series of dichromonyl molecules and found an optically inactive mixture of stereoisomers that exhibited polymorphism, of which rapid cooling resulted in a nematic liquid crystal phase whereas aging at ambient temperature resulted in precipitation. This mixture consists of three stereoisomers: a pair of enantiomers (52%), 5'DSCG-(*R,R*)-diviol and 5'DSCG-(*S,S*)-diviol, and an achiral compound (48%), 5'DSCG-*meso*-diviol.²² The precipitates obtained after aging overnight were comprised of a mixture

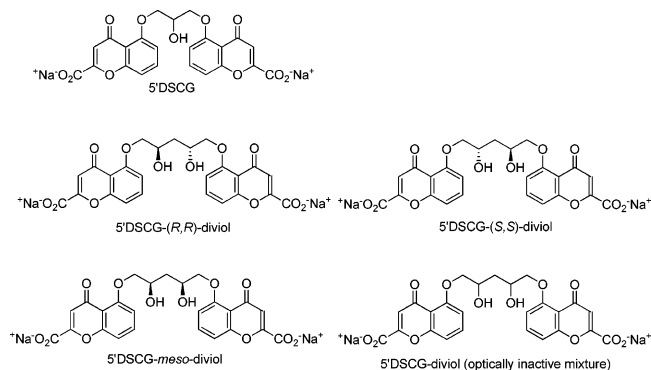
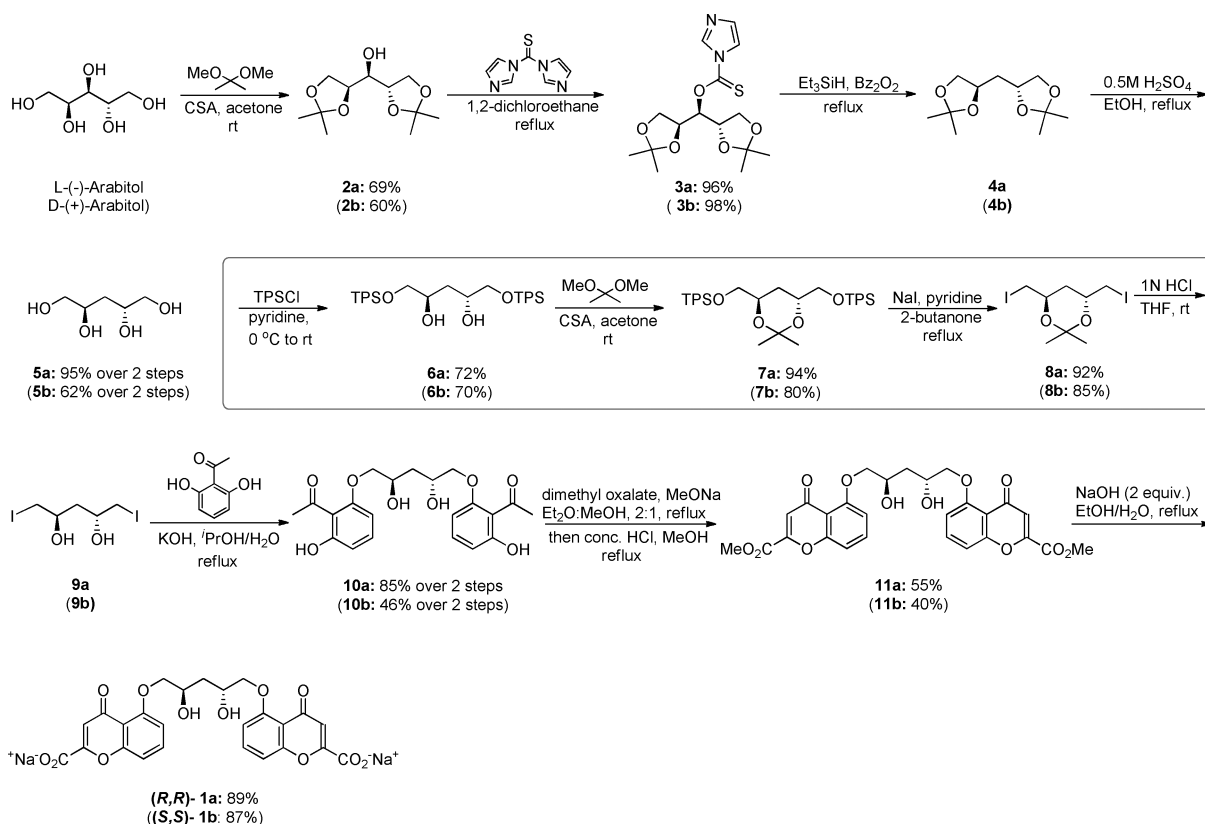


Figure 1. Structures of 5'DSCG, chiral isomers 5'DSCG-(*R,R*)-diviol and 5'DSCG-(*S,S*)-diviol, achiral isomer 5'DSCG-*meso*-diviol, and the optically inactive mixture which contains 52% of a racemic mixture of (*R,R*) and (*S,S*) isomers and 48% of meso compounds.

Scheme 1. Synthesis of 5'DSCG-(*R,R*)-Diviol 1a and 5'DSCG-(*S,S*)-Diviol 1b



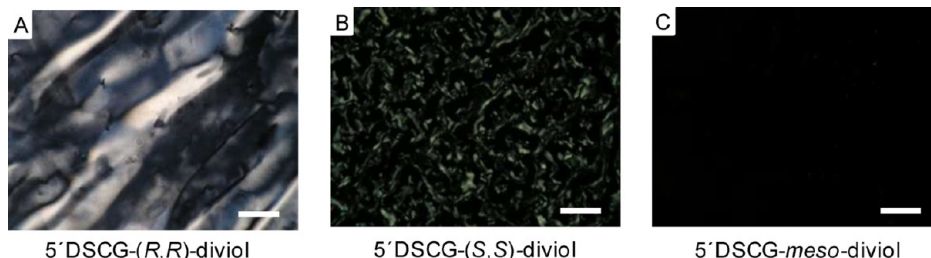
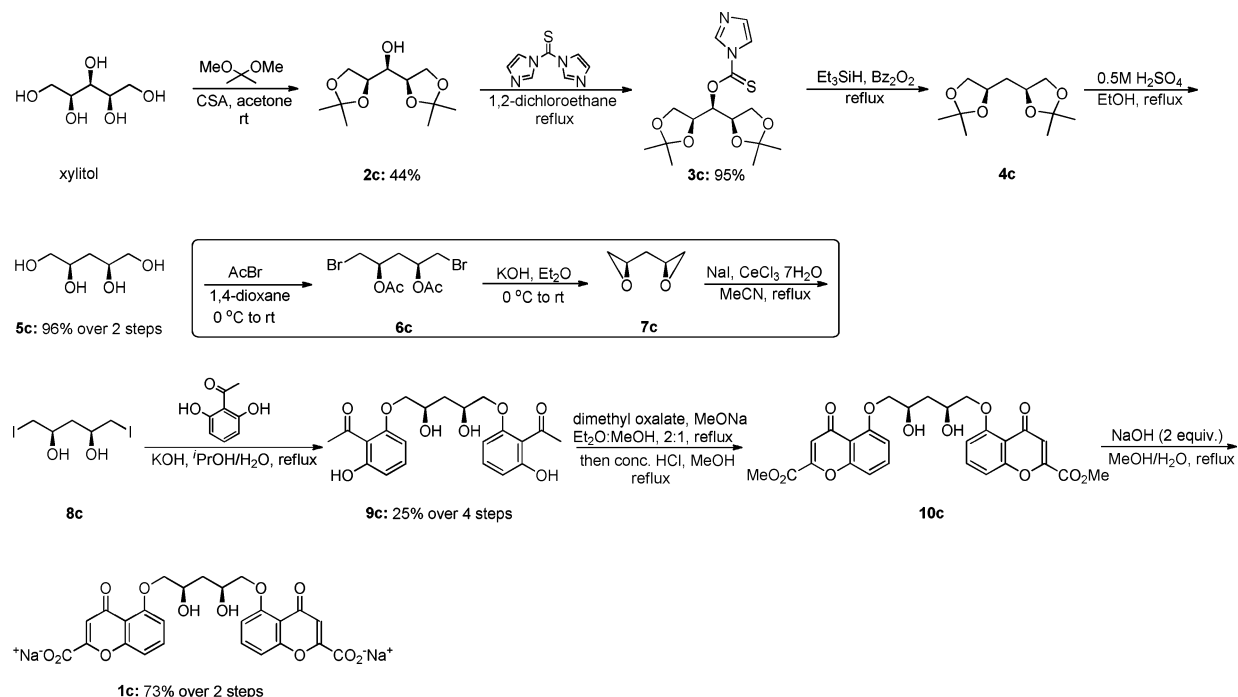
Scheme 2. Synthesis of 5'DSCG-*meso*-Diviol 1c

Figure 2. Optical images (cross polarizers) of 12.0 wt % 5'DSCG-(*R,R*)-diviol (A), 5'DSCG-(*S,S*)-diviol (B), and 5'DSCG-*meso*-diviol (C) in water sandwiched between two glass slides (spacer: 13–15 μm). Samples were freshly prepared by dissolving solid in water at ambient temperature. Scale bar = 76 μm .

of all three stereoisomers, and thus spontaneous resolution^{36,37} was not achieved. To study the effect of stereochemistry on assembly and liquid crystal formation, we synthesize each stereoisomer individually.

The synthesis of the chiral isomers 5'DSCG-(*R,R*)-diviol and 5'DSCG-(*S,S*)-diviol was done using the same route (Scheme 1) but started with L-(−)-arabitol and D-(+)-arabitol, respectively. Briefly, 2,4-dihydroxypentane-1,5-diyl bis-(2,4,6-triisopropyl-1-benzenesulfonate) **6a** was obtained in 5 steps starting from L-(−)-arabitol.³⁸ Acetonization of bis-sulfonate **6a** followed by iodination and deacetonization provided diiodo diol **9a** which was treated directly with an excess of 2,6-dihydroxyacetophenone to give the substitution adduct **10a**. A two-step cyclization sequence from modified conditions³⁹ built the chromonyl ring of diester **11a**. First, hydroxyl ketone **10a** was added to a mixture of sodium methoxide and dimethyl oxalate in a solvent mixture of Et_2O and MeOH (2:1 by volume) and the reaction mixture was refluxed overnight. Acidification of the reaction mixture gave a yellow precipitate. Second, the yellow precipitate was treated with concentrated hydrochloric acid under reflux in methanol to give dichromonyl ester **11a**. We note that the use of this mixed solvent system was critical for obtaining useful yields. Basic hydrolysis of

dichromonyl ester **11a** with a stoichiometric amount of sodium hydroxide provided the final product 5'DSCG-(*R,R*)-diviol **1a**.

Using xylitol as the starting material to attain the desired *meso* stereochemistry, 5'DSCG-*meso*-diviol was synthesized with a modified synthetic route from that for the chiral stereoisomers (Scheme 2) because the same route was not effective for the *meso* isomer. The different steps included acetyl-bromination of tetraol **5c** to give bromoacetate **6c**,⁴⁰ epoxidation under basic conditions to generate diepoxide **7c** that was purified by bulb-to-bulb distillation,⁴¹ and iodination of diepoxide **7c** to give diiodo diol **8c**. Compound **8c** was used to obtain the final product **1c** under the same reaction conditions as that for the chiral isomers. We note that, although the chiral diester **11a** or **11b** (for the chiral isomers) precipitated out from the reaction mixture, most of the achiral diester **10c** remained in the solution (Scheme 2).

Stereochemistry Controls the Formation of Liquid Crystals. To examine the potential liquid crystal properties, samples of each stereoisomer in water were sandwiched between two microscope glass slides with one sheet of Saran Wrap (13–15 μm thick) as a spacer. A square hole of $\sim 0.5 \times 0.5$ cm was cut in the sheet of Saran Wrap to host the sample. Binder clips were applied on each side to prevent the

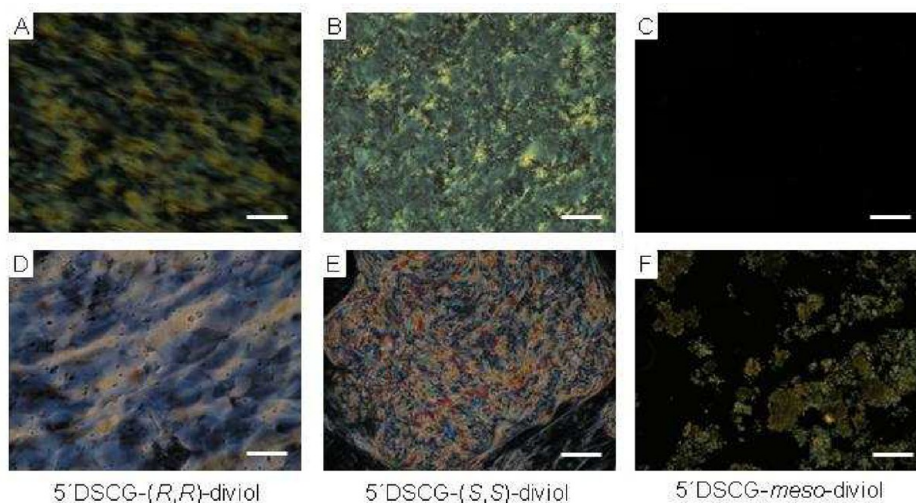


Figure 3. Optical images (cross polarizers) of 18.0 wt % 5'DSCG-(*R,R*)-diviol, 18.1 wt % 5'DSCG-(*S,S*)-diviol, and 18.0 wt % 5'DSCG-*meso*-diviol in water when freshly prepared (A, B, and C, respectively) and when aged at ambient temperature overnight in sealed vials (D, E, and F, respectively). The samples are sandwiched between two glass slides with a spacer of 13–15 μm thick. Scale bar = 76 μm .

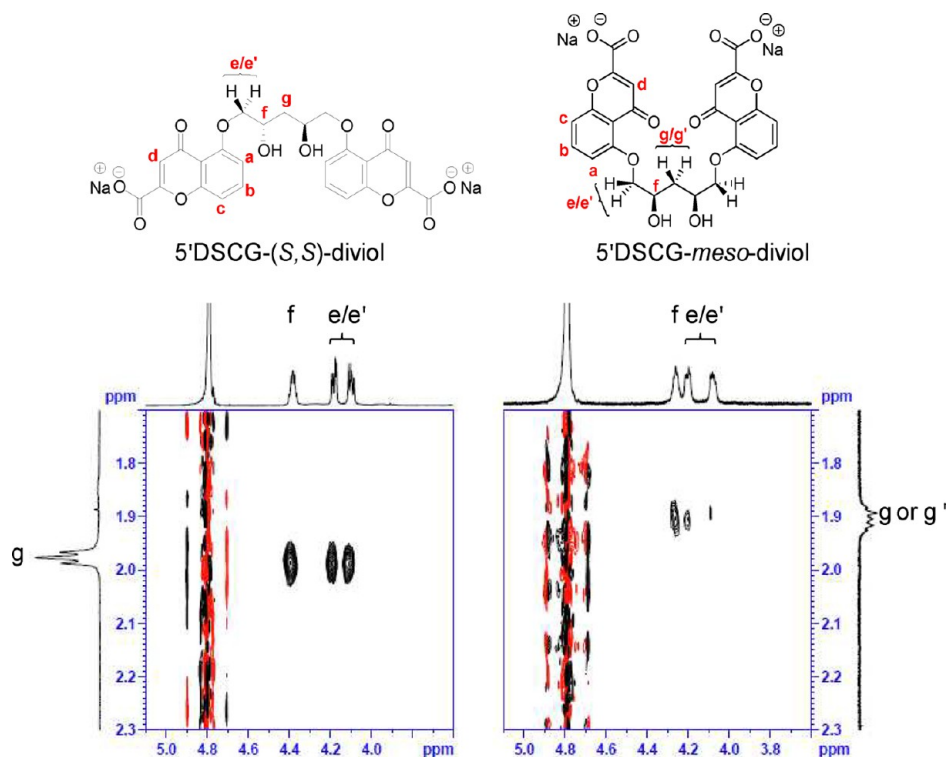


Figure 4. ROESY of 0.503 wt % of 5'DSCG-(*S,S*)-diviol and 0.503 wt % of 5'DSCG-*meso*-diviol in D_2O at 25 $^{\circ}\text{C}$.

evaporation of solvent. Between cross polarizers, 5'DSCG-(*R,R*)-diviol exhibited birefringence at a concentration as low as 12.0 wt % (with a mole ratio of water to mesogen of 226:1) at ambient temperature, about 21 $^{\circ}\text{C}$ (Figure 2A). At the same concentration (12.0 wt %), 5'DSCG-(*S,S*)-diviol showed a liquid crystal phase at 18 $^{\circ}\text{C}$ (Figure 2B). We believed that this difference in phase behavior between the (*R,R*) and (*S,S*) isomers may be caused by the miniscule difference in purity such as small amounts of salts that are beyond the measurement of NMR. Salts are known to change the nematic–isotropic transition temperature of liquid crystals formed by 5'DSCG.³² The achiral stereoisomer 5'DSCG-*meso*-diviol at the same concentration (12.0 wt %) showed a mixture

of isotropic solution and a small amount of insoluble solid (Figure 2C). Furthermore, rapid cooling did not induce liquid crystal formation in this sample. This result indicates that 5'DSCG-*meso*-diviol is either less capable or incapable of forming liquid crystals, which likely contributes to the fact that the mixture of all three stereoisomers requires a lower temperature or a higher concentration than the individual chiral stereoisomers to form a liquid crystal phase. We note that 5'DSCG-*meso*-diviol has lower water solubility than the chiral isomers 5'DSCG-(*R,R*)-diviol and 5'DSCG-(*S,S*)-diviol.

Stereoisomers of 5'DSCG-Diviols Exhibit Different Polymorphism. To explore liquid crystal formation without any cooling, we prepared 18.0 wt % 5'DSCG-(*R,R*)-diviol and

18.1 wt % 5'DSCG-(*S,S*)-diviol (Figure 3A,B). Both of these chiral 5'DSCG-diviols exhibited birefringence over the entire sample prepared at ambient temperature. In contrast, 5'DSCG-*meso*-diviol at this concentration resulted in an isotropic solution with insoluble solids. Rapid cooling of this sample did not induce liquid crystal formation. After aging overnight at ambient temperature in vials sealed with parafilm to prevent evaporation, we observed that the chiral and *meso* 5'DSCG-diviol resulted in different assemblies. The sample of 18.0 wt % 5'DSCG-(*R,R*)-diviol became a mixture of liquid crystals with small precipitates, whereas 18.1 wt % 5'DSCG-(*S,S*)-diviol remained a mixture of liquid crystals and isotropic solution (Figure 3D,E). Under the same conditions, 18.0 wt % of 5'DSCG-*meso*-diviol in water remained a mixture of isotropic solution and aggregates (Figure 3F). In comparison, the polymorphism of the individual enantiomer was different from that observed in the earlier work of an optically inactive mixture of all three stereoisomers (a mixture of 52% racemic mixture and 48% *meso* isomer): a freshly prepared sample of 18.0 wt % of mesogens transitioned from an isotropic solution to liquid crystal phase by rapid cooling to 15 °C without observable precipitates, whereas isothermal aging gives precipitates in isotropic solution. Together, these results suggest that, for the optically inactive mixture,²² the liquid crystal phase represents a local energy minimum, and the precipitation in isotropic solution is of a global minimum in the energy profile.

Conformations of Stereoisomers. Diastereomers may or may not be of grossly different conformation. In the proton NMR spectra, differences in the chemical shifts of the diviol linker in the chiral and *meso* 5'DSCG-diviol suggest that the conformations between these diastereomers are different from each other (see Figure S1). To access the conformations of the diastereomers and their differences, we used two-dimensional NMR spectroscopy to characterize the conformations of the (*S,S*) isomer and the *meso* isomer. Because the *meso* isomer has a lower solubility than the (*S,S*) isomer in water, we believe that even with a concentration at which both molecules appear to dissolve in D₂O, the dynamics of the two molecules in solution may not be the same. For this reason, we focused on using ROESY to characterize the structure to avoid the potential null of NOE signals due to the dynamics of the molecules.⁴² We observed large differences in the NOE correlations in the ROESY spectra for the diviol bridge region between the two diastereomers in D₂O (Figure 4). For 0.503 wt % of 5'DSCG-(*S,S*)-diviol, NOEs between protons **g** and **e** (and **e'**) and between **g** and **f** were observed with similar peak intensities. This result suggests that these protons (**g** and **e/e'** and **g** and **f**) are in close proximity by similar distances. In contrast, for 5'DSCG-*meso*-diviol at the same wt %, protons **g** and **g'** on the same methylene group were in different chemical environment, and thus exhibited different chemical shifts. More importantly, one of the "**g**" protons showed weak NOE correlation with only one of the "**e**" protons. The other "**g**" proton exhibited NOE correlation with both of the "**e**" protons, with strong and weak NOE signal intensities, respectively (see Figure S2). These NOEs indicate that one of the "**g**" protons was in close proximity to both of the "**e**" protons, whereas the other "**g**" proton was close in space to only one of the "**e**" protons. These results suggest that the diviol region in the *meso* isomer is twisted through certain preferred bond rotation angle. Together, these spacing of protons in the two diastereomers suggests that 5'DSCG-(*S,S*)-diviol likely adopts an average "stretched" conformation while 5'DSCG-*meso*-diviol is more of

a "folded" conformation. These conformational differences also appear to be consistent with the low solubility of the *meso* isomer and the formation of assemblies by the (*S,S*) isomer.

Circular Dichroism Indicates a Chiral Conformation.

Circular dichroism (CD) spectra were collected to examine the chirality of chiral 5'DSCG-diviol at feasible concentrations (0.1 to 0.8 mM). The two enantiomers of 5'DSCG-diviol showed CD spectra with mirror signals having a minimum and maximum at 274 and 339 nm (Figure 5A). Considering the

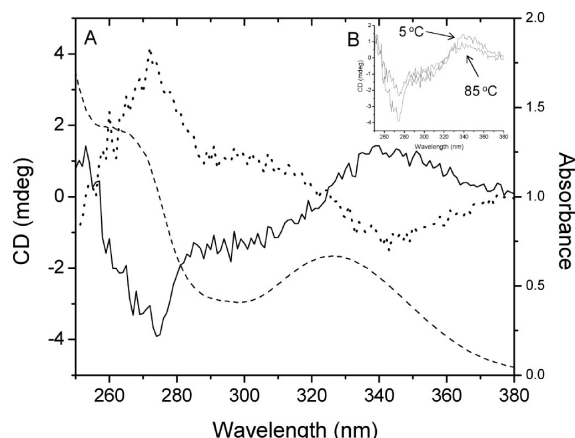


Figure 5. (A) UV spectrum of 5'DSCG-(*R,R*)-diviol (dash line) at ambient temperature and CD spectra at 5 °C of 5'DSCG-(*R,R*)-diviol (solid line) and 5'DSCG-(*S,S*)-diviol (dot line) in water (8×10^{-4} M). (B) Temperature-dependent CD spectra of 5'DSCG-(*R,R*)-diviol in water (8×10^{-4} M). Spectra were taken in a 1 mm path length cuvette.

UV absorption at 256 and 325 nm bisignate Cotton effects in the $\pi-\pi^*$ transition were observed in the CD spectra for 5'DSCG-(*R,R*)-diviol (8×10^{-4} M) with a positive effect at 324 nm and a negative effect at 256 nm (Figure 5A). Although the bisignate cotton effect may suggest the presence of ordered chiral assembly,^{4,43} temperature-dependence study (Figure 5B) showed an insignificant decrease in the intensity of CD signal as the temperature increased to 85 °C. Furthermore, in a concentration-dependent study of the absorbance by 5'DSCG-(*R,R*)-diviol in water, a near constant molar absorptivity was observed at 325 nm in the concentration ranging from 5 μ M to 1.6 mM using 1 mm- and 1 cm-path cuvettes (data not shown). Together, these results suggest that at this concentration range (<1.6 mM) the molecules are mostly in the monomeric (or dimeric) state, and that the chiral conformation is stable at relatively high temperature. However, we have observed significant upfield chemical shift in the proton NMR of 5'DSCG-(*R,R*)-diviol in D₂O from 0.4 to 61 mM, and significant peak broadening from 61 to 72 mM (see Figure S3). This result is consistent with a previous NMR study of the achiral generic 5'DSCG, in which upfield chemical shift and peak broadening were also observed at slightly higher concentration range.⁴⁴

Cryogenic Transmission Electron Microscopy Reveals Early and Crossed Assemblies by Chiral Mesogens.

Cryogenic transmission electron microscopy (cryo-TEM) provides valuable, direct information of the complex nanostructures and microstructures in the solution state. It has been used to characterize the size and shape of peptides, DNA, lipids, viruses, and the self-assembly of polymers, surfactants, and liquid crystals.^{32,45} To access the assembly structure of the chiral mesogens, we compared the cryo-TEM images of the

5'DSCG-(*R,R*)-diol and the generic 5'DSCG at concentrations below and above which assemblies form (Figures 6 and 7). For the full cryo-TEM images (see Figure S4–7).

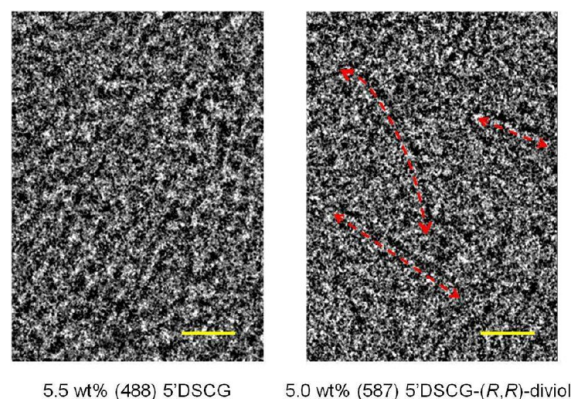


Figure 6. Cryogenic transmission electron microscopy images of 5.5 wt % of 5'DSCG and 5.0 wt % of 5'DSCG-(*R,R*)-diol. Numbers in the parentheses indicate the mole ratio of water and mesogens in the sample. The red dash lines indicate the assembly. Scale bar = 10 nm.

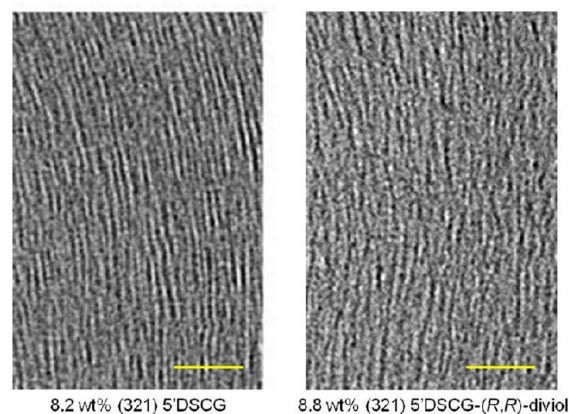


Figure 7. Cryogenic transmission electron microscopic images of 8.2 wt % of 5'DSCG and 8.8 wt % of 5'DSCG-(*R,R*)-diol. Numbers in parentheses indicate the mole ratio of water and mesogens in the sample. Scale bar = 50 nm.

A past study of small angle neutron scattering showed that the assembly structure started to appear for 5'DSCG at about 5–6 wt %.²² Thus, we chose 5'DSCG (5.5 wt %, mole ratio of water molecules to mesogens is 488) and 5'DSCG-(*R,R*)-diol (5.0 wt %, mole ratio of water to mesogen is 587) to compare the early stage features of the molecular assembly. We note that the sample of chiral mesogen 5'DSCG-(*R,R*)-diol had a lower concentration than the one with achiral mesogen 5'DSCG. Interestingly, assemblies were more visible in the 5'DSCG-(*R,R*)-diol samples, whereas mostly blocks of assemblies with about 5–7 nm gap were observed in the 5'DSCG samples (Figure 6). These results indicate that the chiral mesogen 5'DSCG-(*R,R*)-diol can form assemblies at a lower concentration than that by 5'DSCG. At these concentrations, a liquid crystal phase was not observed for either of the samples, and the supramolecular assembly structures appeared to be connected by “blocks” of assemblies. Although supramolecular assemblies were visible in the 5'DSCG-(*R,R*)-diol samples, they were randomly oriented, consistent with a sample of isotropic solution at this concentration.

As the concentration of 5'DSCG-(*R,R*)-diol increased to 8.8 wt %, the assemblies were more elongated and more aligned with each other than those observed in samples at lower concentrations (Figure 7). This elongation of the assemblies as the concentration increases is consistent with the notion of an isodesmic assembly,^{46,47} for which there is no critical concentration for assembly but the observed blocks of assemblies continue to grow to form assembly. The cryo-TEM images also showed that the aligned assembly structures were separated by about 6 nm, and the alignment between the assemblies was uniform over at least hundreds of nanometers. Interestingly, there were more crossings between the assemblies formed by 5'DSCG-(*R,R*)-diol than those formed by 5'DSCG (Figure 7) and that the chiral mesogen exhibited large curvature in the assemblies.

The polymorphism of liquid crystal phases and precipitates under different condition, and the 6 nm-separation between the assemblies as revealed by cryo-TEM suggest that the assemblies in liquid crystals are likely hydrated by solvent water, which prevent aggregation and precipitation for the chiral isomers. This hydration implies a competition between assemblies getting solvated and aggregating with other assemblies. Whereas aggregation of mesogens leads to insoluble precipitation, hydration of assemblies leads to liquid crystal formation. For the polymorphism shown in the optically inactive mixture, we believe that the achiral mesogen is coprecipitating with the chiral stereoisomers, but rapid cooling can condense the readily available water molecules around the newly formed assembly to insulate the assemblies from aggregating, and thus facilitate liquid crystal formation.

Nonuniform Alignment of Liquid Crystals Formed by 5'DSCG-(*R,R*)-Diol in Water. To examine the liquid crystal phases comprised of chiral mesogens, we used a surface that can align the generic 5'DSCG liquid crystal uniformly over a large area²⁵ and explored if a uniform alignment could also be obtained for the liquid crystals formed by the chiral 5'DSCG-(*R,R*)-diol. Any chiral phase of liquid crystals will *not* give a uniform single-colored texture over the entire liquid crystal sample because of the continuous change in the molecular orientation in the chiral nematic phase. Thus, a surface that can align a nematic phase uniformly^{25,48,49} is a useful tool to determine whether a chiral nematic phase exists or not. We have recently reported uniform alignment of 5'DSCG liquid crystal on surfaces presenting self-assembled monolayers (SAMs) of functionalized alkanethiols supported on gold films that were deposited onto glass slides at an incident angle oblique from the surface normal of the glass slides. When sandwiched between two such surfaces, hydrated molecular assemblies of 5'DSCG and Sunset Yellow dye aligned in parallel to the surface of the SAMs, and uniformly in a preferred direction over the entire sample.²⁵

For classical cholesteric liquid crystal samples, the exhibited fingerprint texture can often be observed by chiral mesogens or by achiral mesogens mixed with a chiral dopant. Here, we also compared the liquid crystal formed by chiral 5'DSCG-diols and by achiral 5'DSCG mixed with a small chiral molecule. In this work, using the same surfaces (two SAMs of HS-(CH₂)₁₀(OCH₂CH₂)₃OH on gold films that were deposited with a 45° incident angle),²⁵ 16.8 wt % 5'DSCG in water gave a uniform alignment (see Figure S8A), which exhibited a strong modulation in the intensity of transmitted light when the sample is rotated with respect to either one of the crossed polarizers. Uniform alignment was observed as expected for

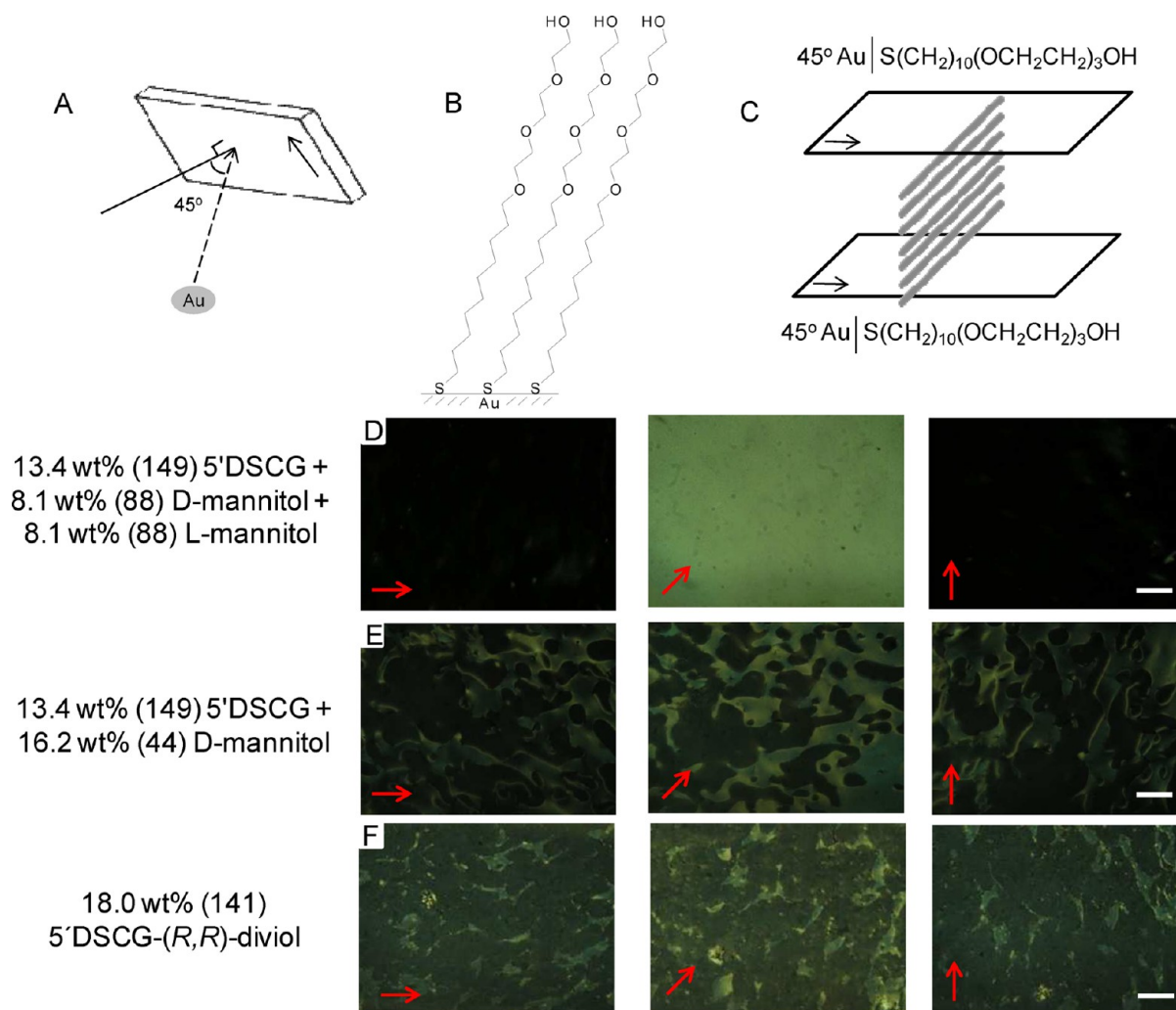


Figure 8. (A) Geometry of gold deposition on glass slides at an oblique angle from the surface normal. (B) Scheme of self-assembly molecules (SAMs) formed by $\text{HS}(\text{CH}_2)_{10}(\text{OCH}_2\text{CH}_2)_3\text{OH}$. (C) Schematic representation of uniform alignment of assemblies of 5'DSCG liquid crystal on SAMs supported by gold films deposited at 45° from the surface normal of the glass slides. Optical images (cross polarizers) of (D) 13.4 wt % 5'DSCG mixed with a 16.2 wt % racemic mixture of D- and L-mannitol, (E) 13.4 wt % 5'DSCG doped with 16.2 wt % D-mannitol, and (F) 18.0 wt % 5'DSCG-(R,R)-diviol in water sandwiched between obliquely deposited gold films supporting $\text{HS}(\text{CH}_2)_{10}(\text{OCH}_2\text{CH}_2)_3\text{OH}$. Numbers in parentheses indicate mole ratio of water and mesogens in the sample. Scale bar = $152\ \mu\text{m}$. The arrows indicate direction of gold deposition projected onto the glass slides, and the orientation of the sample relative to the cross polarizers.

14.1 wt % 5'DSCG mixed with 14.5 wt % achiral molecule xylitol (see Figure S8B). When 13.4 wt % 5'DSCG was mixed with a racemic mixture of D- and L-mannitol (8.1 wt % of each), uniform alignment of liquid crystal phase was observed (Figure 8D). On the contrary, a nonuniform alignment was observed for a sample containing 13.4 wt % 5'DSCG doped with 16.2 wt % enantiomerically pure D-mannitol (Figure 8E). Two domains with different colors that switched between bright and dark were observed as the sample was rotated between the cross polarizers. Using the liquid crystal cell with the same self-assemble monolayers, the 5'DSCG-(R,R)-diviol (18.0 wt %) liquid crystal sample also exhibited similar, nonuniform alignments with two domains of different orientations (Figure 8F). The modulation of transmitted light in these samples was weak when the sample is rotated between the polarizers. This result is consistent with a mixture of liquid crystal orientations of homogeneous planar alignment of a chiral nematic phase and a forced uniform planar alignment induced by the surface. We note that all the samples were warmed to above liquid crystal-

isotropic transition temperature to remove potential effect of viscosity or flow on the liquid crystal alignment.

Chiral Nematic (Cholesteric) Phase Formed by Non-amphiphilic Mesogens. To observe the chiral nematic phase, we reduced the dominating alignment effect of the surface on the interior bulk of the liquid crystal by increasing the thickness of the spacer using a wedge cell. This wedge cell was created by using two different spacers are used, one is a Saran wrap of about $13\ \mu\text{m}$, and the other is a glass slide of about 1 mm thick, this geometry gave a continuous increase in the thickness of the liquid crystal cell (Figure 9A). Figure 9 shows the images of liquid crystal at different thicknesses and different sample orientations relative to the cross polarizers. As the thickness was increased to about 18 and $296\ \mu\text{m}$ (Figure 9B,C), liquid crystal (13.4 wt % 5'DSCG + 16.2 wt % D-mannitol) showed a largely uniform color (yellow and green) throughout the sample. More importantly, when the sample was rotated between the cross polarizers, there was no modulation of light. This result is consistent with a homogeneous chiral nematic phase with uniform planar alignment on the surfaces (Figure 9D).

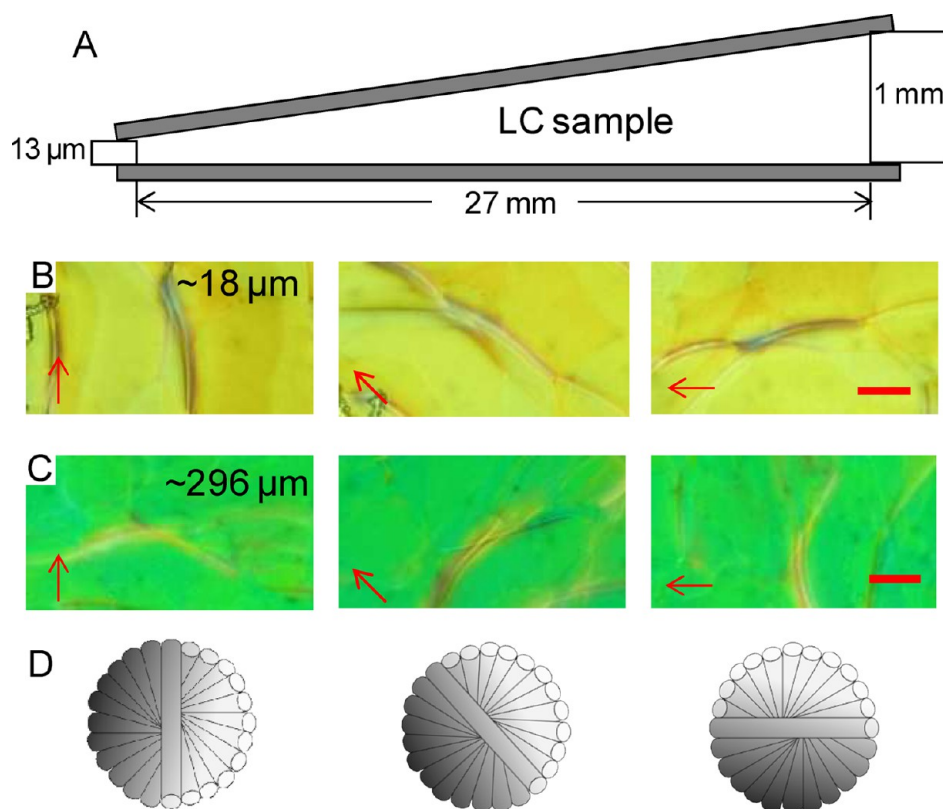


Figure 9. (A) Schematic representation of a wedge cell composed of $\text{HS}(\text{CH}_2)_{10}(\text{OCH}_2\text{CH}_2)_3\text{OH}$ SAMs supported by gold films. Optical images (cross polarizers) of 13.4 wt % 5'DSCG mixed with 16.2 wt % D-mannitol when the thickness of the cell is (B) 18 μm and (C) 296 μm . (D) Schematic representation of the homogeneous planar alignment of the assemblies in the chiral nematic phase, viewed from the top. Scale bar = 76 μm . The arrows indicate direction of gold deposition projected onto the glass slides, and the orient. ation of the sample relative to the cross polarizers.

As the thickness of spacer was increased to about 778 μm , for a sample of 13.4 wt % 5'DSCG mixed with 16.2 wt % D-mannitol, we observed fingerprint texture which is the characteristic feature of a chiral nematic (cholesteric) phase (Figure 10 A). The liquid crystal community has recognized that the vertical alignment (homeotropic alignment) of this

class of liquid crystal is difficult to obtain. Using a liquid crystal cell with 1-mm thick spacer, we also observed fingerprint for the chiral mesogen, 18.0 wt % 5'DSCG-(*R,R*)-diviol in water (Figure 10 B). For a fingerprint alignment of the chiral nematic phase of this class of lyotropic liquid crystals (Figure 10 C), a significant amount of assemblies have to adopt a homeotropic alignment (perpendicular to the surface) and polar alignments (with a polar angle) from the surface. One of the possible mechanisms that facilitate this homeotropic alignment is that as the thickness was increased, the planar anchoring effect of the surface is greatly reduced for the interior bulk of the liquid crystal, allowing the homeotropic alignment formation.

We note that the liquid crystal phase of 13.4 wt % 5'DSCG mixed with 16.2 wt % D-mannitol showed helical pitches of $\sim 25\text{--}28\ \mu\text{m}$. The liquid crystal phase of the chiral mesogen, 18.0 wt % 5'DSCG-(*R,R*)-diviol, showed a helical pitch around 10 μm (Figure 10). Considering the distance between the neighboring thread assembly is $\sim 6\ \text{nm}$ as evidenced in the cryo-TEM, we calculated the degree of twist between two neighboring assemblies in each liquid crystal sample by $360^\circ \times 0.006/p$, where p is the helical pitch in μm . For chiral nematic phase of chiral mesogen, 18 wt % of 5'DSCG-(*R,R*)-diviol, the twist angle between two assemblies is $\sim 0.22^\circ$. For the chiral nematic formed by 13.4 wt % 5'DSCG mixed with 16.2 wt % D-mannitol, the twist angle range from 0.08 to 0.09° . We note that the pitches obtained in our case (10–30 μm) are comparable to the past reported cases of 5'DSCG mixed with chiral molecules (10–100 μm).^{14,61}

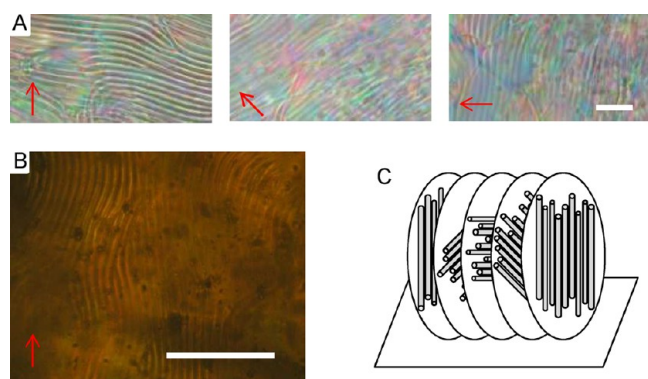


Figure 10. Optical images (cross polarizers) of (A) 13.4 wt % 5'DSCG mixed with 16.2 wt % D-mannitol with 778 μm cell thickness and (B) 18.0 wt % 5'DSCG-(*R,R*)-diviol with 1 mm cell thickness, when the samples were sandwiched between obliquely deposited gold films supporting $\text{HS}(\text{CH}_2)_{10}(\text{OCH}_2\text{CH}_2)_3\text{OH}$. (C) Schematic representations of molecular assemblies in chiral nematic phase. Scale bar = 76 μm . The arrows indicate direction of gold deposition projected onto the glass slides, and the orientation of the sample relative to the cross polarizers.

The above results are all on surfaces that provide uniform planar alignment of liquid crystals (both thermotropic and this class of nonamphiphilic lyotropic liquid crystals). To demonstrate that the chiral nematic phase of this class of liquid crystal can also form on other surfaces, we used plain glass slides in wedge cells. Both planar alignment (with random azimuthal directions) and fingerprint texture were observed for 13.4 wt % 5'DSCG mixed with 16.2 wt % D-mannitol (see Figure S9).

In comparison with the thermotropic liquid crystals, the key question for a chiral nematic phase of a lyotropic liquid crystal is how the chiral information is being transmitted between the assemblies that are separated by a rather large volume of water molecules, more than 80% by weight in the case of chiral mesogen of 5'DSCG-(*R,R*)-diviol. For a thermotropic liquid crystal, the mesogens are in van der Waals contact with each other; and the chiral information is transmitted through dispersion interaction between molecules and manifested by molecules twisting relative to each other continuously throughout each domain in the liquid crystal sample.^{1,9,50,51} In lyotropic liquid crystals, the assemblies are not in direct van der Waals contact with each other, but separated by water solvent molecules. For chiral mesogen in water, we believe that there are three possible modes of chemical information transmission between the assemblies of chiral mesogens in water. First, the assemblies are separated by pure water, and there is no or negligible amount of chiral mesogens. Thus, chiral information is transmitted through an achiral solvent medium. For both isodesmic and cooperative assemblies, this scenario is probable when the self-association constant is high. For a rough estimation in our case, the two neighboring assemblies are separated by at least 14–18 water molecules. This number is estimated by assuming a linear hydrogen bonding arrangement between the water molecules. Second, there may be certain amount of chiral mesogens solvated as individual free molecules in the aqueous solvent between the assemblies. These molecules may function as a chiral dopant to twist the molecular assemblies. This scenario is possible, but the transmission of chiral information is needed to be mediated by the solvent molecules because the free chiral mesogens are still solvated. Third, the chiral mesogens branch out (or grow out) of the assemblies and connect to the neighboring assemblies. Through this connection, the chiral information is somehow transmitted and manifested as twisting neighboring assemblies. This scenario is unlikely because such a cross-linked network will cause gel formation instead of a fluid phase.

In the case of achiral mesogens mixed with chiral molecules in water, the transmission of chemical information is not likely through pure water because of the high concentration of chiral molecules. However, because the chiral molecules are small molecules, the transmission of the chemical information must still go through many molecular interactions between the chiral molecules and the solvent water molecules, and eventually reaching the neighboring assemblies. In an aqueous solution, the hydrogen bonds are ubiquitous. However, it is important to note that the contribution from the dispersion force between the molecules should not be overlooked as they exist independent of the types of functional groups. How exactly the chiral information is transmitted through the solvent is a still an open question.

It is important to note that there are precedents of organized water structures.^{6,52–57} For example, the sucrose density gradients in water that are commonly used for purification of

biomolecules are stable over a long period of time.^{52,53} In such a gradient solution, water molecules between the sucrose molecules are dynamically different across the gradient.⁶ In a recent study using molecular dynamics simulation, water dynamics in the solvation shell of proteins have shown to be different from bulk water. The terahertz spectroscopy data suggested an influence on the correlated water network motion beyond two nm between neighboring proteins.⁵⁵ Our recent work also demonstrated that the stereochemistry of polyol diastereomers on surfaces impacted their ability to resist protein adsorption, mammalian cell adhesion and biofilm formation.⁵⁷ As the atomic composition is the same for those surfaces, this resistance to biofouling is likely due to the templated aqueous solvent structure at the interfaces. Surface force studies on bioinert SAMs by Grunze and co-workers measured force effect as far as more than 10 nm from the surfaces.^{58,59} Finally, using chiral lyotropic liquid crystals as solvents, discrimination of enantiomers can be observed in NMR spectra. These studies suggest that the solvent is promoting a preferred orientation of the solutes.^{54,56}

Together with the anisotropic interactions at the mesoscale, liquid crystal materials can create complex and interesting assembly structures.⁶⁰ With the potential of structuring the organization of water molecules, new assembly in water can be explored.

CONCLUSION

In conclusion, enantiomers of 5'DSCG-(*R,R*)-diviol and 5'DSCG-(*S,S*)-diviol and achiral 5'DSCG-*meso*-diviol were individually synthesized. Chiral stereoisomers formed liquid crystal phases while the *meso* isomer did not. The nuclear Overhauser effect in proton NMR spectroscopy revealed that the 5'DSCG-*meso*-diviol adopted a more “folded” conformation while the chiral 5'DSCG-diviol had a more “stretched” conformation. Circular dichroism suggested a stable chiral molecular conformation by 5'DSCG-(*R,R*)-diviol. Proton NMR revealed significant upfield chemical shift and peak broadening around 72 mM. Cryo-TEM showed visible assembly at 5 wt % (~103 mM) and that chiral stereoisomer 5'DSCG-(*R,R*)-diviol forms more elongated assembly at low concentration in water, and exhibited more crossings between the assemblies at high concentration than those shown by generic 5'DSCG in water. Both achiral 5'DSCG mixed with chiral D-mannitol in water and the chiral mesogen, 5'DSCG-(*R,R*)-diviol, exhibited chiral nematic phases. Together, these results suggest that the hydrated assemblies of chiral molecules 5'DSCG-(*R,R*)-diviol interact with each other while being separated by a relatively large distance (6 nm) in water, causing a continuous twist between the assemblies and forming a chiral nematic phase.

ASSOCIATED CONTENT

Supporting Information

Detailed synthesis procedures, characterization of three stereoisomers of 5'DSCG-diviol, and other experimental details. Additional NMR spectroscopy, cryo-TEM images, and optical images. This material is available free of charge via the Internet at <http://pubs.acs.org>.

AUTHOR INFORMATION

Corresponding Author

*E-mail: yluk@syr.edu.

Notes

The authors declare no competing financial interest.

ACKNOWLEDGMENTS

We thank Dr. S. N. Loh (SUNY-Upstate Medical University) for circular dichroism, Dr. B. S. Hudson (SU) for discussion, and NSF-CMMI (CAREER #0845686) and NSF-11-560 (#1242505) for partial financial support.

REFERENCES

- (1) Gottarelli, G.; Hibert, M.; Samori, B.; Solladie, G.; Spada, G. P.; Zimmermann, R. Induction of the cholesteric mesophase in nematic liquid crystals: mechanism and application to the determination of bridged biaryl configurations. *J. Am. Chem. Soc.* **1983**, *105*, 7318–7321.
- (2) Green, M. M.; Reidy, M. P.; Johnson, R. D.; Darling, G.; O'Leary, D. J.; Willson, G. Macromolecular stereochemistry: the out-of-proportion influence of optically active comonomers on the conformational characteristics of polyisocyanates. The sergeants and soldiers experiment. *J. Am. Chem. Soc.* **1989**, *111*, 6452–6454.
- (3) Brunsveld, L.; Zhang, H.; Glasbeek, M.; Vekemans, J. A. J. M.; Meijer, E. W. Hierarchical Growth of Chiral Self-Assembled Structures in Protic Media. *J. Am. Chem. Soc.* **2000**, *122*, 6175–6182.
- (4) Besenius, P.; Portale, G.; Bomans, P. H. H.; Janssen, H. M.; Palmans, A. R. A.; Meijer, E. W. Controlling the growth and shape of chiral supramolecular polymers in water. *Proc. Natl. Acad. Sci. U.S.A.* **2010**, *107*, 17888–17893.
- (5) Korevaar, P. A.; Schaefer, C.; de Greef, T. F. A.; Meijer, E. W. Controlling Chemical Self-Assembly by Solvent-Dependent Dynamics. *J. Am. Chem. Soc.* **2012**, *134*, 13482–13491.
- (6) Seraydarian, K.; Mommaerts, W. F. Density gradient separation of sarcotubular vesicles and other particulate constituents of rabbit muscle. *J. Cell. Biol.* **1965**, *26*, 641–656.
- (7) Yu, L. J.; Saupe, A. Liquid crystalline phases of the sodium decylsulfate/decanol/water system. Nematic-nematic and cholesteric-cholesteric phase transitions. *J. Am. Chem. Soc.* **1980**, *102*, 4879–4883.
- (8) Kamien, R. D.; Lubensky, T. C. Chiral lyotropic liquid crystals: TGB phases and helicoidal structures. *J. Phys. II* **1997**, *7*, 157–163.
- (9) Hiltrop, K. In *Chirality in Liquid Crystals*; Kitzrow, H.-S., Bahr, C., Eds.; Springer: Seacacus, NJ, 2001; Chapter 14.
- (10) von Minden, H. M.; Vill, V.; Pape, M.; Hiltrop, K. Sugar Amphiphiles as Revealing Dopants for Induced Chiral Nematic Lyotropic Liquid Crystals. *J. Colloid Interface Sci.* **2001**, *236*, 108–115.
- (11) Goodby, J. W. Twist grain boundary and frustrated liquid crystal phases. *Curr. Opin. Colloid Interface Sci.* **2002**, *7*, 326–332.
- (12) Dorfner, H.-D. Chirality, twist and structures of micellar lyotropic cholesteric liquid crystals in comparison to the properties of chiral thermotropic phases. *Adv. Colloid Interface Sci.* **2002**, *98*, 285–340.
- (13) Dawin, U. C.; Dilger, H.; Roduner, E.; Scheuermann, R.; Stoykov, A.; Giesselmann, F. Chiral Induction in Lyotropic Liquid Crystals: Insights into the Role of Dopant Location and Dopant Dynamics. *Angew. Chem., Int. Ed.* **2010**, *49*, 2427–2430.
- (14) Lee, H.; Labes, M. M. Lyotropic cholesteric and nematic phases of disodium cromoglycate in magnetic fields. *Mol. Cryst. Liq. Cryst.* **1982**, *84*, 137–157.
- (15) Lydon, J. Chromonic mesophases. *Curr. Opin. Colloid Interface Sci.* **2004**, *8*, 480–490.
- (16) Nastishin, Y. A.; Liu, H.; Schneider, T.; Nazarenko, V.; Vasyuta, R.; Shiyankovskii, S. V.; Lavrentovich, O. D. Optical characterization of the nematic lyotropic chromonic liquid crystals: Light absorption, birefringence, and scalar order parameter. *Phys. Rev. E* **2005**, *72*, 041711.
- (17) Simon, K. A.; Sejwal, P.; Gerecht, R. B.; Luk, Y.-Y. Water-in-Water Emulsions Stabilized by Non-Amphiphilic Interactions: Polymer-Dispersed Lyotropic Liquid Crystals. *Langmuir* **2007**, *23*, 1453–1458.
- (18) Tomasik, M. R.; Collings, P. J. Aggregation behavior and chromonic liquid crystal phase of a dye derived from naphthalene-carboxylic acid. *J. Phys. Chem. B* **2008**, *112*, 9883–9889.
- (19) Edwards, D. J.; Jones, J. W.; Lozman, O.; Ormerod, A. P.; Sinyureva, M.; Tiddy, G. J. T. Chromonic liquid crystal formation by Edicol Sunset Yellow. *J. Phys. Chem. B* **2008**, *112*, 14628–14636.
- (20) Tam-Chang, S.-W.; Huang, L. Chromonic liquid crystals: properties and applications as functional materials. *Chem. Commun.* **2008**, 1957–1967.
- (21) Park, H.-S.; Kang, S.-W.; Tortora, L.; Nastishin, Y.; Finotello, D.; Kumar, S.; Lavrentovich, O. D. Self-Assembly of Lyotropic Chromonic Liquid Crystal Sunset Yellow and Effects of Ionic Additives. *J. Phys. Chem. B* **2008**, *112*, 16307–16319.
- (22) Wu, L.; Lal, J.; Simon, K. A.; Burton, E. A.; Luk, Y.-Y. Nonamphiphilic Assembly in Water: Polymorphic Nature, Thread Structure, and Thermodynamic Incompatibility. *J. Am. Chem. Soc.* **2009**, *131*, 7430–7443.
- (23) Tortora, L.; Park, H.-S.; Kang, S.-W.; Savaryn, V.; Hong, S.-H.; Kaznatcheev, K.; Finotello, D.; Sprunt, S.; Kumar, S.; Lavrentovich, O. D. Self-assembly, condensation, and order in aqueous lyotropic chromonic liquid crystals crowded with additives. *Soft Matter* **2010**, *6*, 4157–4167.
- (24) McKitterick, C. B.; Erb-Satullo, N. L.; La Racuente, N. D.; Dickinson, A. J.; Collings, P. J. Aggregation Properties of the Chromonic Liquid Crystal Benzopurpurin 4B. *J. Phys. Chem. B* **2010**, *114*, 1888–1896.
- (25) Simon, K. A.; Burton, E. A.; Cheng, F.; Varghese, N.; Falcone, E. R.; Wu, L.; Luk, Y.-Y. Controlling Thread Assemblies of Pharmaceutical Compounds in Liquid Crystal Phase by Using Functionalized Nanotopography. *Chem. Mater.* **2010**, *22*, 2434–2441.
- (26) Simon, K. A.; Sejwal, P.; Falcone, E. R.; Burton, E. A.; Yang, S.; Prashar, D.; Bandyopadhyay, D.; Narasimhan, S. K.; Varghese, N.; Gobalasingham, N. S.; Reese, J. B.; Luk, Y.-Y. Noncovalent Polymerization and Assembly in Water Promoted by Thermodynamic Incompatibility. *J. Phys. Chem. B* **2010**, *114*, 10357–10367.
- (27) Tortora, L.; Lavrentovich, O. D. Chiral symmetry breaking by spatial confinement in tactoidal droplets of lyotropic chromonic liquid crystals. *Proc. Natl. Acad. Sci. U. S. A.* **2011**, *108*, 5163–5168.
- (28) Simon, K. A.; Shetye, G. S.; English, U.; Wu, L.; Luk, Y.-Y. Noncovalent Polymerization of Mesogens Crystallizes Lysozyme: Correlation between Nonamphiphilic Lyotropic Liquid Crystal Phase and Protein Crystal Formation. *Langmuir* **2011**, *27*, 10901–10906.
- (29) Varghese, N.; Shetye, G. S.; Bandyopadhyay, D.; Gobalasingham, N.; Seo, J.; Wang, J.-H.; Theiler, B.; Luk, Y.-Y. Emulsion of Aqueous-Based Nonspherical Droplets in Aqueous Solutions by Single-Chain Surfactants: Templated Assembly by Nonamphiphilic Lyotropic Liquid Crystals in Water. *Langmuir* **2012**, *28*, 10797–10807.
- (30) Mills, E. A.; Regan, M. H.; Stanic, V.; Collings, P. J. Large Assembly Formation via a Two-Step Process in a Chromonic Liquid Crystal. *J. Phys. Chem. B* **2012**, *116*, 13506–13515.
- (31) Prasad, S. K.; Nair, G. G.; Hegde, G.; Jayalakshmi, V. Evidence of Wormlike Micellar Behavior in Chromonic Liquid Crystals: Rheological, X-ray, and Dielectric Studies. *J. Phys. Chem. B* **2007**, *111*, 9741–9746.
- (32) Kostko, A. F.; Cipriano, B. H.; Pinchuk, O. A.; Ziserman, L.; Anisimov, M. A.; Danino, D.; Raghavan, S. R. Salt Effects on the Phase Behavior, Structure, and Rheology of Chromonic Liquid Crystals. *J. Phys. Chem. B* **2005**, *109*, 19126–19133.
- (33) Lee, H.; Labes, M. M. Phase diagram and thermodynamic properties of disodium cromoglycate-water lyomesophases. *Mol. Cryst. Liq. Cryst.* **1983**, *91*, 53–58.
- (34) Lavrentovich, M.; Sergan, T.; Kelly, J. Planar and twisted lyotropic chromonic liquid crystal cells as optical compensators for twisted nematic displays. *Liq. Cryst.* **2003**, *30*, 851–859.
- (35) Lydon, J. Chromonic liquid crystal phases. *Curr. Opin. Colloid Interface Sci.* **1998**, *3*, 458–466.
- (36) Walba, D. M.; Korblova, E.; Shao, R.; MacLennan, J. E.; Link, D. R.; Glaser, M. A.; Clark, N. A. A ferroelectric liquid crystal

- conglomerate composed of racemic molecules. *Science* **2000**, *288*, 2181–2184.
- (37) Takezoe, H. Spontaneous achiral symmetry breaking in liquid crystalline phases. *Top. Curr. Chem.* **2012**, *318*, 303–330.
- (38) Linclau, B.; Boydel, A. J.; Clarke, P. J.; Horan, R.; Jacquet, C. Efficient De-Symmetrization of "Pseudo"-C₂-Symmetric Substrates: Illustration in the Synthesis of a Disubstituted Butenolide from Arabitol. *J. Org. Chem.* **2003**, *68*, 1821–1826.
- (39) Walenzyk, T.; Carola, C.; Buchholz, H.; Koenig, B. Chromone derivatives which bind to human hair. *Tetrahedron* **2005**, *61*, 7366–7377.
- (40) Terauchi, T.; Terauchi, T.; Sato, I.; Tsukada, T.; Kanoh, N.; Nakata, M. Synthetic studies on althoyrtins (spongistatins): synthesis of the C15–C28 (CD) spiroacetal portion. *Tetrahedron Lett.* **2000**, *41*, 2649–2653.
- (41) Rychnovsky, S. D.; Griesgraber, G.; Zeller, S.; Skaltitzky, D. J. Optically pure 1,3-diols from (2R,4R)- and (2S,4S)-1,2:4,5-diepoxy-pentane. *J. Org. Chem.* **1991**, *56*, 5161–5169.
- (42) Bauer, C. J.; Frenkiel, T. A.; Lane, A. N. A comparison of the ROESY and NOESY experiments for large molecules, with application to nucleic acids. *J. Magn. Reson.* **1990**, *87*, 144–152.
- (43) Langeveld-Voss, B. M. W.; Beljonne, D.; Shuai, Z.; Janssen, R. A. J.; Meskers, S. C. J.; Meijer, E. W.; Bredas, J.-L. Investigation of exciton coupling in oligothiophenes by circular dichroism spectroscopy. *Adv. Mater.* **1998**, *10*, 1343–1348.
- (44) Ding, X.; Stringfellow, T. C.; Robinson, J. R. Self-association of cromolyn sodium in aqueous solution characterized by nuclear magnetic resonance spectroscopy. *J. Pharm. Sci.* **2004**, *93*, 1351–1358.
- (45) Zhong, S.; Pochan, D. J. Cryogenic Transmission Electron Microscopy for Direct Observation of Polymer and Small-Molecule Materials and Structures in Solution. *Polym. Rev.* **2010**, *50*, 287–320.
- (46) Maiti, P. K.; Lansac, Y.; Glaser, M. A.; Clark, N. A. Isodesmic self-assembly in lyotropic chromonic systems. *Liq. Cryst.* **2002**, *29*, 619–626.
- (47) Smulders, M. M. J.; Nieuwenhuizen, M. M. L.; de Greef, T. F. A.; van der Schoot, P.; Schenning, A. P. H. J.; Meijer, E. W. How to Distinguish Isodesmic from Cooperative Supramolecular Polymerisation. *Chem.—Eur. J.* **2010**, *16*, 362–367.
- (48) Gupta, V. K.; Abbott, N. L. Design of surfaces for patterned alignment of liquid crystals on planar and curved substrates. *Science* **1997**, *276*, 1533–1536.
- (49) Luk, Y.-Y.; Tingey, M. L.; Hall, D. J.; Israel, B. A.; Murphy, C. J.; Bertics, P. J.; Abbott, N. L. Using liquid crystals to amplify protein-receptor interactions: Design of surfaces with nanometer-scale topography that present histidine-tagged protein receptors. *Langmuir* **2003**, *19*, 1671–1680.
- (50) Green, M. M.; Zanella, S.; Gu, H.; Sato, T.; Gottarelli, G.; Jha, S. K.; Spada, G. P.; Schoevaars, A. M.; Feringa, B.; Teramoto, A. Mechanism of the Transformation of a Stiff Polymer Lyotropic Nematic Liquid Crystal to the Cholesteric State by Dopant-Mediated Chiral Information Transfer. *J. Am. Chem. Soc.* **1998**, *120*, 9810–9817.
- (51) Wulf, A. Distribution function theory of nematic liquid crystals. *J. Chem. Phys.* **1971**, *55*, 4512–4519.
- (52) Brakke, M. K. Density gradient centrifugation: a new separation technique. *J. Am. Chem. Soc.* **1951**, *73*, 1847–1848.
- (53) Svensson, H.; Valmet, E. Large-scale density-gradient electrophoresis. II. A simple experimental technique for securing perfectly stable zones and full utilization of the separation capacity of a density-gradient column. *Sci. Tools* **1959**, *6*, 13–17.
- (54) Sarfati, M.; Lesot, P.; Merlet, D.; Courtieu, J. Theoretical and experimental aspects of enantiomeric differentiation using natural abundance multinuclear NMR spectroscopy in chiral polypeptide liquid crystals. *Chem. Commun.* **2000**, 2069–2081.
- (55) Ebbinghaus, S.; Kim, S. J.; Heyden, M.; Yu, X.; Heugen, U.; Gruebele, M.; Leitner, D. M.; Havenith, M. An extended dynamical hydration shell around proteins. *Proc. Natl. Acad. Sci. U.S.A.* **2007**, *104*, 20749–20752.
- (56) Lesot, P.; Lafon, O.; Zimmermann, H.; Luz, Z. Enantiodiscrimination in Deuterium NMR Spectra of Flexible Chiral Molecules with

Average Axial Symmetry Dissolved in Chiral Liquid Crystals: The Case of Tridioxymethylenetriphenylene. *J. Am. Chem. Soc.* **2008**, *130*, 8754–8761.

(57) Bandyopadhyay, D.; Prashar, D.; Luk, Y.-Y. Anti-Fouling Chemistry of Chiral Monolayers: Enhancing Biofilm Resistance on Racemic Surface. *Langmuir* **2011**, *27*, 6124–6131.

(58) Feldman, K.; Haehner, G.; Spencer, N. D.; Harder, P.; Grunze, M. Probing Resistance to Protein Adsorption of Oligo(ethylene glycol)-Terminated Self-Assembled Monolayers by Scanning Force Microscopy. *J. Am. Chem. Soc.* **1999**, *121*, 10134–10141.

(59) Skoda, M. W. A.; Schreiber, F.; Jacobs, R. M. J.; Webster, J. R. P.; Wolff, M.; Dahint, R.; Schwendel, D.; Grunze, M. Protein Density Profile at the Interface of Water with Oligo(ethylene glycol) Self-Assembled Monolayers. *Langmuir* **2009**, *25*, 4056–4064.

(60) Poulin, P.; Stark, H.; Lubensky, T. C.; Weitz, D. A. Novel colloidal interactions in anisotropic fluids. *Science* **1997**, *275*, 1770–1773.

(61) Park, H.-S.; Lavrentovich, O. D. In *Liquid Crystals Beyond Displays: Chemistry, Physics, and Applications*; Li, Q., Ed.; John Wiley & Sons: Hoboken, NJ, 2012; Chapter 14.